Fluorescence emission induced by extensive air showers in dependence on atmospheric conditions

Bianca Keilhauer*, Michael Unger*

**Karlsruhe Institute of Technology (KIT),*
Forschungszentrum Karlsruhe, Institut für Kernphysik, P.O.Box 3640, 76021 Karlsruhe, Germany

***Abstract*. Charged particles of extensive air showers (EAS), mainly electrons and positrons, initiate the emission of fluorescence light in the Earth's atmosphere. This light provides a calorimetric measurement of the energy of cosmic rays. For reconstructing the primary energy from an observed light track of an EAS, the fluorescence yield in air has to be known in dependence on atmospheric conditions, like air temperature, pressure, and humidity. Several experiments on fluorescence emission have published various sets of data covering different parts of the dependence of the fluorescence yield on atmospheric conditions.**

Using a compilation of published measurements, a calculation of the fluorescence yield in dependence on altitude is presented. The fluorescence calculation is applied to simulated air showers and different atmospheric profiles to estimate the influence of the atmospheric conditions on the reconstructed shower parameters.

***Keywords*: atmosphere-dependent fluorescence emission, temperature-dependent collisional cross sections, vapour quenching**

I. Introduction

The number of emitted fluorescence photons at the air shower can be written as

$$\frac{d^2N_\gamma^0}{dX\,d\lambda} = Y(\lambda, P, T, e) \cdot \frac{dE_{\rm dep}^{\rm tot}}{dX}, \tag{1}$$

where $Y(\lambda, P, T, e)$ is the fluorescence yield in dependence on wavelength λ, air pressure P, air temperature T, and vapour pressure e. The deposited energy of the secondary particles is denoted as $dE_{\rm dep}^{\rm tot}/dX$.

In the last couple of years, a lot of effort has been put on the investigation of atmospheric dependences on nitrogen fluorescence in air [1]. The fluorescence yield Y_λ can be written as

$$Y_\lambda = \Phi_\lambda^0 \cdot \lambda/hc \cdot \frac{1}{1 + P/P_v'}, \tag{2}$$

where Φ_λ^0 is the fluorescence efficiency at zero pressure, P is the air pressure, and P' is the characteristic pressure for which the probability of collisional quenching equals that of radiative de-excitation. The index v indicates the vibrational level of the exited state. Several groups have already investigated aspects of the fluorescence emission from nitrogen molecules in air (e.g. Bunner [2], Davidson & O'Neil [3], Kakimoto et al. [4], MACFLY [5] and FLASH [6]). In addition there are various ongoing experimental activities, e.g. AIRFLY [7], [8], [9], [10], Nagano & Sakaki et al. [11], [12], AirLight [13] and Ulrich & Morozov et al. [14]. One major goal of all experiments is to obtain an absolute fluorescence yield $Y_\lambda^0 = \Phi_\lambda^0 \cdot \lambda/hc$ either for the main contributing band at 337.1 nm or for the entire spectrum in the range of interest between about 300 – 420 nm. Y_λ^0 represents the intrinsic radiative de-excitation of the nitrogen molecules. However, in gas like air quenching processes have to be taken into account because the rate of radiative de-excitations is reduced by collisions between excited nitrogen molecules and further molecules in the gas. These quenching processes depend on atmospheric conditions and are described by $(1+P/P_v')^{-1}$ in Eq. (2). Accounting all currently known effects, we can write

$$\begin{aligned}\frac{P}{P_v'} = {} & \frac{\tau_{0,v} \cdot P_{\rm air} \cdot N_A}{R \cdot T_{\rm air}} \cdot \sqrt{\frac{k \cdot T_{\rm air} \cdot N_A}{\pi}} \\ & \cdot \Bigg(4C_{\rm vol}({\rm N_2}) \cdot \sigma_{{\rm NN},v}(T) \sqrt{M_{\rm N}^{-1}} \\ & + 2C_{\rm vol}({\rm O_2}) \cdot \sigma_{{\rm NO},v}(T) \sqrt{2\Big(M_{\rm N}^{-1} + M_{\rm O}^{-1}\Big)} \\ & + 2C_{\rm vol}({\rm H_2O}) \cdot \sigma_{{\rm NH_2O},v}^0 \sqrt{2\Big(M_{\rm N}^{-1} + M_{\rm H_2O}^{-1}\Big)} \Bigg),\end{aligned} \tag{3}$$

with $\tau_{0,v}$ as the mean life time of the radiative transition to any lower state, the index v indicates again the vibrational level of the exited state as for P_v', N_A is Avogadro's number, R is the universal gas constant, $T_{\rm air}$ is the air temperature, k is the Boltzmann constant, $C_{\rm vol}$ is the fractional part per volume of the relevant gas constituents, and M_x is the mass per mole where x stands for the relevant gas constituents. Up to now, the collisional cross sections $\sigma_{{\rm N}x,v}$ have been taken as temperature-independent even though it was known from theory that there has to be a temperature dependence. Recently, first experiments could confirm this dependence for nitrogen-nitrogen and nitrogen-oxygen quenching. The temperature-dependence of the nitrogen-vapour quenching has not been measured yet. First estimates indicate only minor importance with an effect of less than 1% change in the reconstructed energy of an air shower [15]. An independent measurement of the temperature-dependent collisional cross sections in air has been performed quite recently. First analyses of data indicate compatible results with the measurements from AIRFLY and will be published soon [15].

Adopting this description of fluorescence emission for air shower reconstruction, we have to apply atmospheric profiles for temperature, pressure, and vapour pressure. This cannot be provided by simple atmospheric models as these usually do not include vapour profiles. However, profiles obtained with meteorological radio soundings do provide all necessary quantities [16].

II. Fluorescence Models in Reconstruction

For this study, we could use the simulation and reconstruction framework Offline [17] of the Pierre Auger Observatory [18]. Within this framework, we could obtain standard monthly models for the area of that observatory which do not include water vapour profiles [16]. Additionally, we had access to 109 actual nightly atmospheric profiles from local radio soundings that cover all conditions within a year. One of the advantages of the framework is that it features many implementations of different fluorescence models which can easily be interchanged.

The first implementation of a fluorescence model in Offline, referred to as K96, is based on measurements by Kakimoto et al. [4]. The fluorescence yield is parametrised in dependence on deposited energy and on altitude by considering the pressure and $\sqrt{T}$-dependences. The second fluorescence model, N04, has the same functional form of parametrisation and describes data from Nagano et al. [19], [11]. These measurements provide spectrally resolved data for 15 wavelengths between 300 and 430 nm. Also in this description, only the pressure and $\sqrt{T}$-dependences are considered. The third fluorescence description in Offline is given by the AIRFLY Collaboration in 2007, labelled with A07. The fluorescence yield is given as [9]

$$Y_\lambda(P,T) = Y^{337}_{P_0,T_0} \cdot I^\lambda_{P_0,T_0} \cdot \frac{1+\frac{P_0}{P'(\lambda,T_0)}}{1+\frac{P_0}{P'(\lambda,T_0)\sqrt{T/T_0}}}. \quad (4)$$

$Y^{337}_{P_0,T_0}$ is the fluorescence yield at 337.1 nm as measured at their standard experimental conditions which are P_0 = 800 hPa and T_0 = 293 K. The other transitions have been measured relatively to that at 337.1 nm and are given by $I^\lambda_{P_0,T_0}$. Overall, 34 transitions could be resolved between 295 and 430 nm. Since the absolute calibration of this experiment is still under study, Y_{337} is normalised to the corresponding value of N04. It should be pointed out that the description in this model can easily be expanded to account for vapour quenching and temperature-dependent collisional cross sections. The fourth implementation of a fluorescence model follows the calculation from Keilhauer et al. in 2008 [20]. Here, 23 wavelengths between 300 and 430 nm are considered by applying Eq. (2) and (3). The model uses a compilation of different measurements [20], [21]. For the temperature-dependent collisional cross sections, the data from AIRFLY [9] are used. These α-coefficients are obtained in air, so the same α_λ is applied to NN-collisions and NO-collisions. The temperature-dependent collisional cross sections in Eq. (3) are written as $\sigma_{\mathrm{N}x,\nu}(T) = \sigma^0_{\mathrm{N}x,\nu} \cdot T^{\alpha_\nu}$ where $\sigma^0_{\mathrm{N}x,\nu} = \sigma_{\mathrm{N}x,\nu} \cdot 293^{-\alpha_\nu}$ is the measured temperature-independent cross section at standard experimental conditions of T = 293 K. Cross sections for nitrogen - water vapour collisions have been measured by two experiments [22], [23].

III. Atmosphere-dependent Fluorescence Emission

To study the overall effect of different fluorescence models on reconstructed air shower observables, primary energy E and position of shower maximum $X_{\max}$, it is important to account for only that part of the fluorescence spectrum that a detector is sensitive to as well as the wavelength dependent attenuation in the atmosphere (see for instance Fig. 8d in [11]). Moreover, since the atmospheric parameters P, e and T depend on altitude, different fluorescence models will propagate differently to E and $X_{\max}$ if the shower reached its maximum high in the atmosphere or close to the ground.

To include all these effects, we proceeded as follows: Proton and iron showers with energies between $10^{17.5}$ and 10^{20} eV were generated using Conex [24] and QGSJETII [25]. The fluorescence light was generated according to the K08 model including water vapour quenching and temperature-dependent collisional cross sections. The events were generated with time stamps that corresponds to nights with balloon launches, such that realistic profiles for P, e and T could be obtained. In the following, we will compare the difference in the reconstructed E and $X_{\max}$ values of these simulated showers.

A. Fluorescence Models

The $X_{\max}$ and energy differences for reconstructions with different fluorescence models is shown in Fig. 1. For this figure, the water vapour quenching and temperature-dependent collisional cross sections were *not* switched on in the K08-model, thus this comparison is only sensitive to the $Y(P,T)$ implementations. As explained above, the A07 model is normalised to N04, therefore they are not independent and show correspondingly the smallest differences.

B. Temperature-dependent collisional cross sections and vapour quenching

The influence of the water vapour quenching (σ_e) and temperature-dependent collisional cross sections (σ_T) on $X_{\max}$ and E was studied by subsequently switching off the effects in the reconstruction using the K08-model. As can be seen in the left panel of Fig. 2, ignoring σ_e- and σ_T-effects leads to an underestimation of the reconstructed energy by about 5%. Both σ_e- and σ_T-dependences affect the shape of the longitudinal profile. Since the σ_e-dependence is most important close to ground and the σ_T-dependence affects mainly higher altitudes, the two effects partially compensate (see right

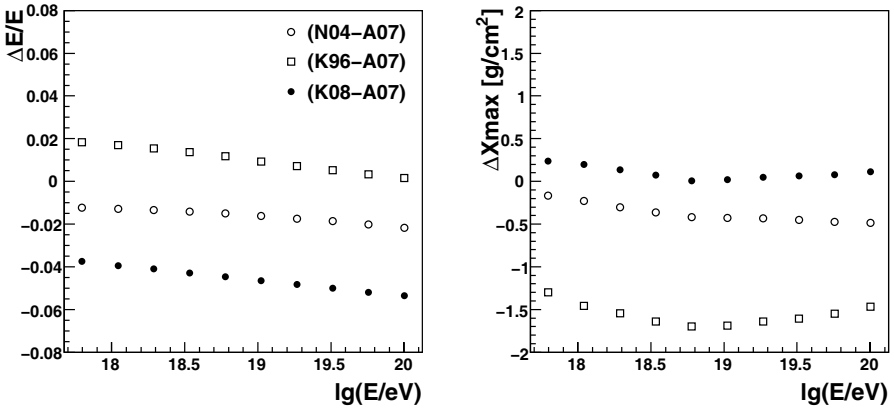

Fig. 1. Comparison of the influence of different fluorescence models on E and $X_{\max}$ (without vapour quenching and temperature-dependent collisional cross sections). The abbreviations of the different fluorescence models are defined in Sec. II.

panel of Fig. 2) leading to only a small $X_{\max}$ shift of $\leq$ 2 g cm^{-2}.

Interchanging the water vapour quenching from [22] with the independent measurement from [23] affects the shower observables very little (see solid black dots in Fig. 2).

The varying strengths of the σ_e- and σ_T-dependences at different altitudes can be seen in Fig. 3. Ignoring the σ_T-effect, the energy is misreconstructed up to -7% for showers with $X_{\max}$ high up in the atmosphere. Ignoring the σ_e-dependence, the energy is underestimated also up to 7% for showers with $X_{\max}$ close to ground. The position of shower maximum is also affected with the largest biases being observed for deep and shallow showers. The overall shift of $X_{\max}$ is strongest for showers with a position of shower maximum at about 3 km a.s.l. with -5 g cm^{-2} or for showers with $X_{\max}$ at 9 km a.s.l. with 5 g cm^{-2}. It can clearly be seen in the right-hand plot of Fig. 3 that the σ_e-dependence cancels out partly the σ_T-dependence concerning $X_{\max}$.

IV. Discussion of Results

In the fluorescence model K08, all currently known effects of the fluorescence light emission are included in dependence on varying atmospheric conditions. Running this model in combination with actual atmospheric profiles, gives a good estimate of the overall misreconstruction and uncertainties of a standard reconstruction. However, it must be stressed that all of the models used in this study have a reported uncertainty of the absolute fluorescence yield well above 10%. In particular, the AIRFLY and AirLight experiments will perform an absolute fluorescence yield calibration with higher accuracy and results can be expected within one year.

In Fig. 4, the difference of the reconstruction of E and $X_{\max}$ using the K08 model with all effects in combination with actual atmospheric profiles and a standard reconstruction with the A07 fluorescence model with monthly models can be seen. More or less independent of energy, the reconstructed primary energy E is higher by about 5% using K08 compared with A07 model. The position of shower maximum $X_{\max}$ is nearly unaffected. These results are very similar to the comparison of the full K08 model and that without σ_e- and σ_T-dependences. Thus, no additional systematics are introduced while changing the fluorescence model apart from those obtained by the σ_e- and σ_T-dependences.

Studying the variation in E and $X_{\max}$ in dependence on the height of the shower maximum, two extreme cases can be found: The average shift in E can be up to -7% for E and -5 g cm^{-2} for $X_{\max}$ for deeply-penetrating showers and up to -7% for E and +5 g cm^{-2} for $X_{\max}$ for showers that develop high in the atmosphere.

Furthermore, we studied the influence of different types of primary particle in terms of proton- and iron-induced showers. Comparing the widths of the distribution, no difference could be found between proton- and iron-induced air showers.

The change in the atmosphere description from monthly models to actual sounding profiles do hardly affect the reconstructed energy nor the position of shower maximum. For E, the difference is well below 1% and for $X_{\max}$ below 2 g cm^{-2}.

Obviously, the fluctuation of the atmosphere around the monthly average atmosphere values adds an additional contribution to the statistical uncertainty of the reconstructed energy and $X_{\max}$ of one shower. The 'end-to-end' comparison of the A07 model with monthly averages to the K08 model with sounding data yields RMS$(\Delta E/E) \in [1.5, 3.0]$% and RMS$(X_{\max}) \in [7.2, 8.4]$ g cm^{-2}(cf. Fig. 4).

Finally, the systematic difference in the collisional cross section data from two independent measurements [22], [23] are negligible. The reconstructed energy varies less than 1% and the position of shower maximum about 1 g cm^{-2} while interchanging the cross sections. Varying the α-coefficients for the temperature-dependent collisional cross sections within their given uncertainties, yields in less than 1% change in reconstructed energy as well.

Acknowledgements

The authors would like to thank the Pierre Auger Collaboration for providing the simulation and reconstruction framework used in this work. Part of this work is supported by the BMBF under contract 05A08VK1.

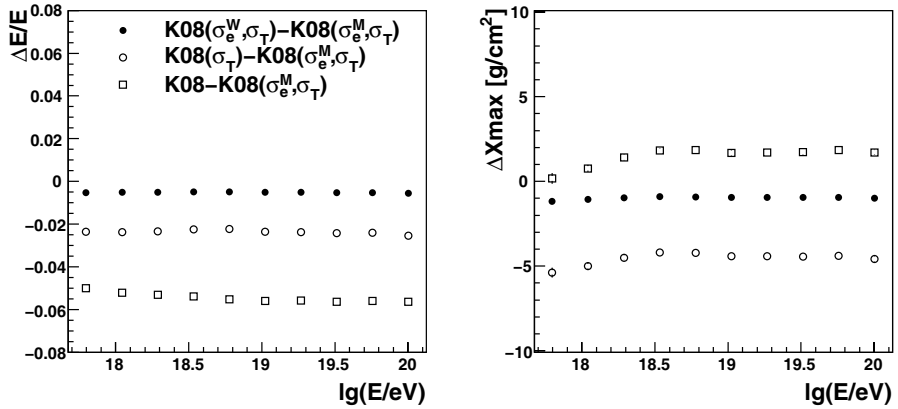

Fig. 2. Comparison of the effect of switching off σ_e and the collisional cross sections σ_T on E and $X_{\max}$ as well as the influence of different vapour quenching, σ_e^W [23] and σ_e^M [22].

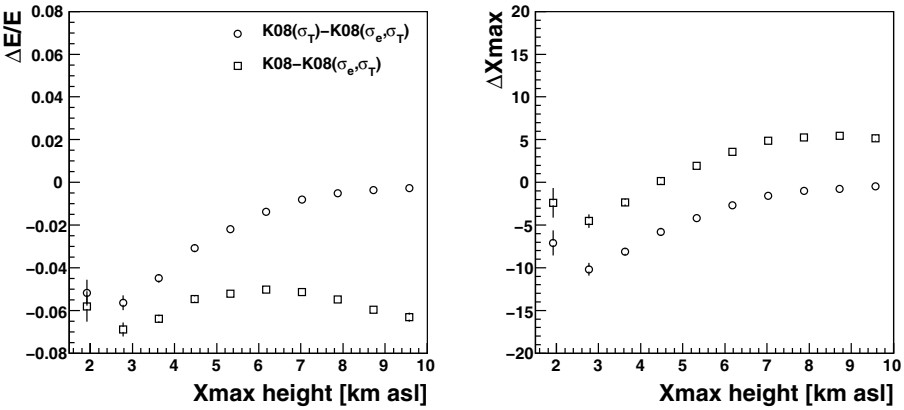

Fig. 3. Difference in reconstructed energy and $X_{\max}$ in dependence the vertical height of the shower maximum ($E = 10^{19}$ eV).

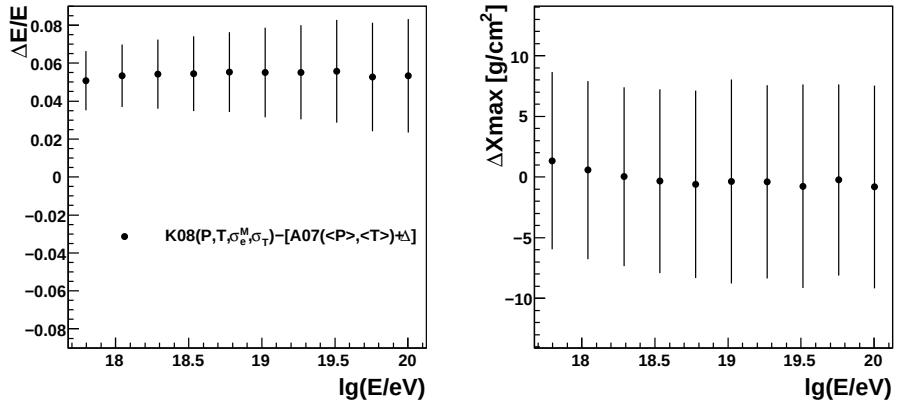

Fig. 4. Difference of the reconstruction using the full K08 model to A07. Error bars denote the RMS spread. Note that we corrected for the 'trivial' yield difference, Δ, from Fig. 1.

REFERENCES

[1] F. Arqueros, J. Hörandel, B. Keilhauer, Nucl. Instr. Meth. **A 597** (2008) 1
[2] A.N. Bunner, Cosmic ray detection by atmospheric fluorescence, Ph.D. Thesis, Cornell University, 1967
[3] G. Davidson, R. O'Neil, J. Chem. Phys. **41** (1964) 3946; R. O'Neil, G. Davidson, American Science and Engineering, Inc., Report AFCRL-67-0277, Cambridge, MA, 1968
[4] F. Kakimoto *et al.*, Nucl. Instr. Meth. **A 372** (1996) 527
[5] P. Colin *et al.* [MACFLY Coll.], Astropart. Phys. **27** (2007) 317
[6] R. Abbasi *et al.* [FLASH Coll.], Nucl. Instr. Meth. **A 597** (2008) 32 and 37
[7] M. Ave *et al.* [AIRFLY Coll.], ibid., 41
[8] M. Ave *et al.* [AIRFLY Coll.], ibid., 46
[9] M. Ave *et al.* [AIRFLY Coll.], ibid., 50
[10] M. Ave *et al.* [AIRFLY Coll.], ibid., 55
[11] M. Nagano *et al.*, Astropart. Phys. **22** (2004), 235
[12] N. Sakaki *et al.*, Nucl. Instr. Meth. **A 597** (2008), 88
[13] T. Waldenmaier *et al.*, ibid., 67
[14] A. Morozov *et al.*, ibid., 105
[15] A. Ulrich, private communication (2009)
[16] B. Keilhauer *et al.*, for the Pierre Auger Collaboration, Proc. 29th Int. Cos. Ray Conf., Pune, India, **7** (2005) 123
[17] S. Argiro *et al.*, Nucl. Instr. Meth. **A580** (2007) 1485; L. Prado *et al.*, Nucl. Instrum. Meth. A **545** (2005) 632
[18] J. Abraham *et al.* [Pierre Auger Coll.], Nucl. Instr. Meth. **A523** (2004) 50
[19] M. Nagano *et al.*, Astropart. Phys. **20** (2003), 293
[20] B. Keilhauer *et al.*, Nucl. Instr. Meth. **A 597** (2008) 99
[21] B. Keilhauer *et al.*, Astropart. Phys. **25** (2006) 259
[22] A. Morozov *et al.*, Eur. Phys. J. **D 33** (2005) 207
[23] T. Waldenmaier, J. Blümer, H. Klages, Astropart. Phys. **29** (2008) 205
[24] T. Bergmann *et al.*, Astropart. Phys. **26** (2007) 420.
[25] S. Ostapchenko, Nucl. Phys. Proc. Suppl. **151**, 143 (2006).